

# High Wear Resistance of White Cast Iron Treated by Novel Process: Principle and Mechanism



XIAOSHUAI JIA, XUNWEI ZUO, YU LIU, NAILU CHEN, and YONGHUA RONG

Based on microstructure desired, a novel process is proposed to treat Fe-2.4C-12.0Cr (mass pct) white cast iron balls, that is, destabilizing heat treatment following multicycle quenching and sub-critical treatment (De-MQ-Sct) process, and such a complex process is simply performed by alternate water quenching and air cooling. For comparison, the white cast iron balls also were treated by conventional normalization (NOR) process and Oil-quenching process, respectively. The partitioning of carbon from martensite to retained austenite during De-MQ-Sct process promotes the interaction between carbide precipitation and martensitic transformation, while this interaction is a unique effect only produced by multicycle quenching linking destabilizing and sub-critical treatments, which leads to more and finer secondary carbides and more carbon-enriched austenite in De-MQ-Sct sample than those in NOR or Oil-quenching sample. The average hardness of 60 HRC and impact toughness of 12.6 J/cm<sup>2</sup> are obtained in De-MQ-Sct white cast iron balls, which are much higher than those in NOR and Oil-quenching ones. The wear behaviours measured by pin-on-disk wear tests indicate that the weight loss of De-MQ-Sct sample is only about one third of the NOR sample and one half of the Oil-quenching sample. Microstructural characterization reveals that high wear resistance related to hardness and toughness of the De-MQ-Sct balls are mainly attributed to the considerable fine secondary carbides and stable carbon-enriched retained austenite.

DOI: 10.1007/s11661-015-3137-4

© The Minerals, Metals & Materials Society and ASM International 2015

## I. INTRODUCTION

HIGH-CHROMIUM white irons are usually hypoeutectic ones, and they are often applied in heavy abrasion condition, such as mineral processing, cement production and steel manufacturing industries, and so on.<sup>[1-5]</sup> Their excellent wear resistance is mainly attributed to the type, amount, morphology and distribution of the carbides and also to the matrix microstructure.<sup>[1,4-7]</sup> The addition of chromium can form considerable carbides in casting irons.<sup>[4]</sup> Additionally, some carbide-forming elements such as cerium, vanadium, boron, titanium, and tungsten can generate the refined secondary carbides, thereby to enhance the abrasion resistance.<sup>[8-12]</sup> The usual production route of high-chromium white irons is usually casting. In the as-cast condition, the network distribution of coarse eutectic M<sub>7</sub>C<sub>3</sub> type carbides is inevitably formed during solidification and leads to poor fracture properties and relatively high wear rate.<sup>[5,13,14]</sup> Moreover, the network eutectic carbides are very stable so that they are not easily eliminated by heat treatment.<sup>[3,15]</sup> Therefore, the microstructure of high-chromium white irons is improved by various heat treatment methods, such as destabilization heat treatment and sub-critical heat

treatment.<sup>[5,16-19]</sup> Destabilizing heat treatment with relative low austenitizing temperature is used to cause coarse secondary carbides to precipitate,<sup>[15]</sup> which lowers the alloy content in austenite and leads to the martensitic transformation at room temperatures if cooling is fast enough.<sup>[5]</sup> While sub-critical heat treatment below austenitizing temperature is to reduce the retained austenite amount and obtain martensitic matrix by the precipitation of considerable fine secondary carbides.<sup>[18,20]</sup> To obtain more martensite, the sub-critical treatment following deep cryogenic treatment was sometime also used.<sup>[20]</sup> However, sub-critical treatment needs long holding time to sufficiently precipitate secondary carbides from austenite so that maximum hardness can be obtained.<sup>[19,21]</sup> The retained austenite has a high intrinsic fracture toughness<sup>[22]</sup> and transformation-induced plasticity (TRIP) by strain-induced martensitic transformation,<sup>[16,17]</sup> such as wear induced martensitic transformation.<sup>[18]</sup> However, it is easy to cause high phase-transformation stress and cracking during the transformation induced by wear.<sup>[19]</sup> It has been verified that the secondary carbides play an important role in determining the mechanical properties and wear resistance of high-chromium white irons.<sup>[3,23-25]</sup> For the above heat treatments, rapid cooling is necessary for white cast irons to avoid the formation of pearlite as possible, which is unfavorable for the wear resistance. However, because white cast irons have casting defects (such as gas porosities, inclusions) and undesirable residual stress, rapid cooling is most likely to cause the cracking. As a result, air cooling (normalization) or Oil-quenching are usually

XIAOSHUAI JIA and YU LIU, PhD Students, XUNWEI ZUO, Engineer, and NAILU CHEN and YONGHUA RONG, Professors, are with the School of Materials Science and Engineering, Shanghai Jiao Tong University, Shanghai 200240, China. Contact e-mail: nlchen@sjtu.edu.cn

Manuscript submitted February 8, 2015.

Article published online September 10, 2015

applied so as to avoid cracking during heat treatment, but the air cooling rate usually cannot markedly improve the hardness and/or toughness of hypoeutectic cast irons in comparison with cast irons,<sup>[21]</sup> while oil cooling leads to the air pollution. Recently, a novel process is proposed based on microstructure desired, that is, destabilizing heat treatment following multicycle quenching and sub-critical treatment (De-MQ-Sct) process. Such a complex process is simply performed by alternate water quenching and air cooling.<sup>[21]</sup> Water and air used in De-MQ-Sct process are the lowest cost and the cleanest cooling media in nature. Because any cooling rates between water and air can be obtained by controlling various ratios of water quenching time and air cooling time,<sup>[26]</sup> they can be used to replace oil, salt, or the aqueous polymer quenchant in heat treatments. The partitioning of carbon from martensite to retained austenite during multicycle water quenching and air cooling (self-tempering) in De-MQ-Sct process promotes the interaction between carbide precipitation and martensitic transformation, leading to more and finer secondary carbides and more carbon-enriched austenite in De-MQ-Sct sample than those in sample treated by normalization (NOR) process, and thus higher hardness and toughness of De-MQ-Sct sample are obtained.<sup>[21]</sup> It is worthy to point out that such an interaction is a unique effect only produced by multicycle quenching linking destabilizing and sub-critical treatments.

The aim of study is to clarify the design principle of novel De-MQ-Sct process based on microstructure desired and to reveal the mechanism of high wear resistance of Fe-2.4C-12.0Cr (mass pct) white cast irons by compared with conventional NOR process and Oil-quenching process.

## II. EXPERIMENTAL PROCEDURES

High-chromium white iron balls with diameter of 80 mm, provided by DeXing Casting Co. LTD of Jiangxi Copper Corporation, were cast from 1823 K (1550 °C) by chilled molds.

The NOR or Oil-quenching process is austenitizing at 1223 K (950 °C) for two hours followed by air cooling or oil cooling, respectively. Combination with destabilizing heat treatment and sub-critical one, the De-MQ-Sct process is designed as follows. The balls are subjected to destabilizing treatment, namely, austenitizing at 1223 K (950 °C) for two hours, being the same as NOR process and Oil-quenching ones. After that, a white cast iron ball will be slowly cooled from 1223 K (950 °C) to near 1073 K (800 °C) by air cooling, and during cooling coarse secondary chromium carbides will precipitate, but the transformation of austenite to pearlite should be as far as possible avoided. The lowering of austenite temperature can decrease subsequent quenching stress. Then, the first water quenching makes the temperature of the ball lower to about 873 K (600 °C), following air cooling for about 50 seconds. The goal is to form martensite at the surface layers of the ball by transformation of austenite to martensite and precipitation of  $M_7C_3$  secondary chromium carbides

from austenite. Subsequently, the second water quenching is performed and makes the temperature of the balls lower to about 673 K (400 °C), following air cooling for a relative long time. The goal is to form martensite at sub-surface layer of the ball and to precipitate more and finer secondary carbides from austenite. Finally, the third water quenching is performed to obtain more martensite by transformation of greater supercooled austenite, and the following air cooling make the temperature of the ball fall to room temperature, during which martensitic transformation still can occur. Figure 1(a) schematically describes De-MQ-Sct process. The De-MQ-Sct process designed is recognized by temperature measurement with WRNK-101 model thermocouple inserted, respectively, at the center and 10 mm from the surface of the ball, as the measured cooling curves shown in Figure 1(b). As comparisons, the cooling curves at the same positions of balls treated, respectively, by NOR process and Oil-quenching process were also demonstrated in Figure 1(b). It can be found from Figure 1(b) that the cooling rates of Oil-quenching process and De-MQ-Sct process are very close, and their cooling rates are much greater than that of NOR process.

After heat treatment, discal samples with a diameter of 80 mm for hardness test and samples with a dimension of  $10 \times 10 \times 55 \text{ mm}^3$  without groove for Charpy impact test were prepared by cutting balls along their radial directions. The HRC hardness was measured using a Rockwell hardness tester with a load of 150 kg, and the impact toughness was measured with PTM2200-D1 impact testing machine.

Friction wear tests were conducted using a computer-aided pin-on-disk wear testing machine, and weight loss was measured to evaluate the wear resistance. The schematic illustration of the wear test is shown in Figure 2. During the wear test, the samples were fixed to the rotating holder and rotated against a WC-Co grinding ball with 5 mm diameter which is fastened to the loading beam through the gripper, while the loads were regulated by the weight of the loadings. The cylindrical test samples with 25 mm diameter and 3 mm thickness were prepared at the positions of surface, 0.5 radius (0.5R) and center of white cast iron balls. Prior to testing, the samples were polished with 400 mesh SiC emery paper to obtain good contact with the WC-Co grinding ball. The wear tests were performed with a constant normal load of 30 N in air at room temperature for three hours without a lubricant, and total wear distance and rotation speed were 3670 m and 650 rpm, respectively. After the wear tests, the weight loss of the samples was measured by a scales with an accuracy of  $\pm 0.0001 \text{ g}$ , and the average value of three measurements was performed on each sample. The worn surfaces were observed by a scanning electron microscope (SEM) after the wear test. The transmission electron microscope (TEM) samples of worn surface were prepared and examined in a JEM 2100 microscope (JEOL) at an operating voltage of 200 kV. The variation of martensite amount before and after wear test is determined by means of magnetic method with Physical Property Measurement System (PPMS-9T (EC-II)). The PPMS samples were cut from both the worn and non-worn areas, and then mechanical

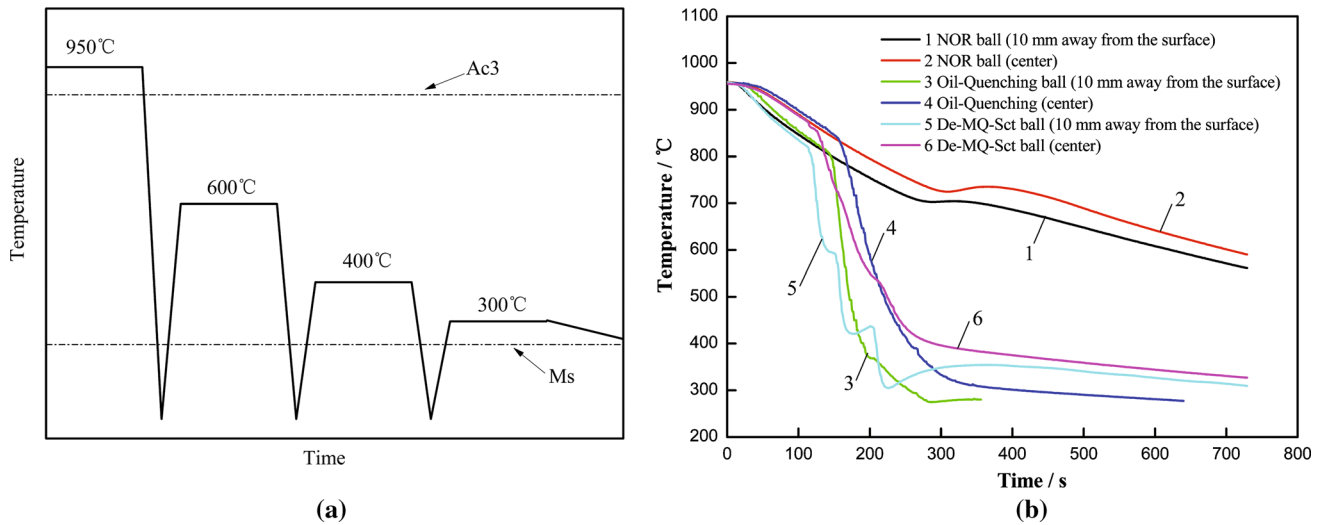


Fig. 1—(a) Schematic illustration of De-MQ-Set process; (b) Cooling curves measured at different positions of white cast iron balls treated, respectively, by three processes.

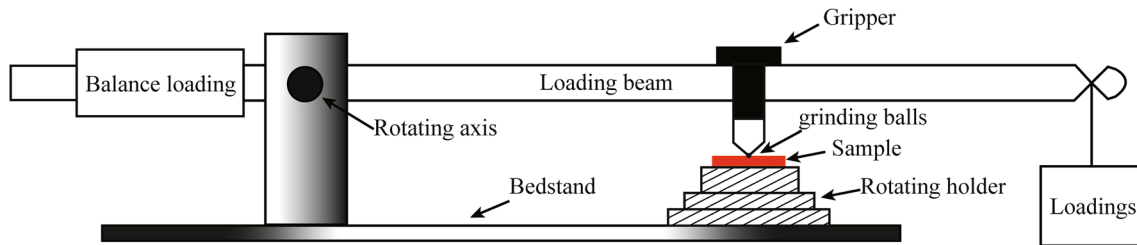


Fig. 2—Schematic illustration of the friction wear testing machine.

grounded to a size of 1 mm × 1 mm × 0.1 mm. The measuring temperature was regulated at 300 ± 0.05 K.<sup>[27]</sup>

The microstructure of samples after mechanical tests was also characterized by X-ray diffraction (XRD), optical microscope (OM), respectively. The XRD was performed in a D/max 2550 X-ray diffraction analyzer at 35 kV and 200 mA with a scanning speed of 2 deg/minute over a 2θ range of 35 to 110 deg using Cu Kα X-ray source and a nickel filter. Since no enough parameters in ASTM cards can be used to calculate the volume percent of eutectic carbide or secondary carbide (M<sub>7</sub>C<sub>3</sub>) based on XRD spectra, Image-Pro Plus software was used to calculate the average volume percent of M<sub>7</sub>C<sub>3</sub> eutectic carbide, M<sub>7</sub>C<sub>3</sub> secondary carbide, MC<sub>3</sub> alloy cementite or pearlite at 0.5 R position of the balls based on 20 SEM photographs, respectively. After that, a XRD spectrum is used to determine the volume percent of a fcc austenite phase or a bcc phase by comparing the integrated intensity of (200) austenite peak with those of bcc (200) and (211) peaks,<sup>[28]</sup> in which the reflections of bcc martensite and bcc ferrite in pearlite are partially or completely overlapped, making their analysis virtually impossible, and thus their fractions are considered as a bcc phase fraction in XRD and Image-Pro Plus software statistics, the volume percent of ferrite is calculated out from that of pearlite

according to lever law of ferrite and MC<sub>3</sub>, and in turn the volume percent of martensite is obtained as balance of a bcc phase. The samples of OM and SEM were polished, then etched in 4 pct Nital solution, and they were observed in a Nikon ECLIPSE MA200 optical microscopy and in a FEI SIRION 200 scanning electron microscopy operating at 10 kV, respectively. Samples for TEM observation were prepared by sectioning into slices with a thickness of about 300 μm and manually grinding down to 80 μm thick slices. Disks, 3 mm in diameter, were punched out and then grinded down to 40 μm foils. Subsequently, these foils were electro-polished at 248 K (−25 °C) in a MTP-1A twin-jet polisher using the electrolyte consisted of 8 pct perchloric acid and 92 pct ethanol solution for 120 seconds, followed by zone thinning in Gatan ion milling instrument at an operating tilt angle of ±4 deg for about 7 hours. The samples were examined in a JEM 2100 microscope (JEOL) at an operating voltage of 200 kV.

### III. RESULTS

#### A. Quantitative Analysis of Phases and Microstructural Characterization

Combining the results of XRD and Image-Pro Plus software statistics, the amount of phases was determined

and given in Table I. Figure 3 shows the XRD spectra of samples treated by De-MQ-Sct, Oil-quenching, and NOR processes, respectively. Phases of hcp  $M_7C_3$ , orthogonal  $MC_3$  carbide, fcc austenite, and bcc lattice structure (ferrite and martensite) were detected. However, diffraction peaks of austenite cannot be observed in the NOR sample, and the diffraction peak of  $MC_3$  cannot be observed in Oil-quenching sample. Besides, austenite completely transforms to pearlite in NOR process, and thus the volume percent of pearlite is high up to 73.0 deg. In Oil-quenching sample there is no pearlite due to without  $MC_3$ . However, the pearlite also forms in De-MQ-Sct process since the two stages of air cooling, respectively, at the sub-critical temperatures about 873 K and 673 K (600 °C and 400 °C), and the volume percent of pearlite is 13.8 pct. It is clearly to see that the amount of  $M_7C_3$  eutectic carbides in the samples treated by the three different processes is close owing to the same austenitizing temperature. It is worth noticing that the volume percent of  $M_7C_3$  secondary carbide in the De-MQ-Sct sample is 13.0 pct, being near one and a half times and twice as in the Oil-quenching and NOR samples, respectively. However, the volume percent of martensite in the Oil-quenching sample is 65.1 pct, being the largest amount in three kinds of samples. It is worthy to point out that in the De-MQ-Sct sample the volume percent of retained austenite is high up to 12.2 pct, being much more than 8.5 pct in Oil-quenching sample.

The microstructures of NOR, Oil-quenching, and De-MQ-Sct samples were characterized, respectively, by OM and SEM, as shown in Figure 4. The microstructure of 0.5 R position of NOR sample is shown in Figures 4((a) and (b)), and that of Oil-quenching sample in Figures 4((c) and (d)) and that of De-MQ-Sct sample in Figures 4((e) and (f)). The optical photograph in Figure 4(a) shows the dendrites with deep gray contrast and bone-like eutectic carbides with bright contrast between dendrites in NOR sample, in which dendrites come from the transformation of proeutectic austenite. The optical photographs of the Oil-quenching (Figure 4(c)) and De-MQ-Sct (Figure 4(e)) samples shows similar morphologies with NOR sample, namely, the network eutectic carbides sketch the dendritic morphology of proeutectic austenite, and the secondary carbides with bright contrast distribute in matrix, as marked by arrows in Figures 4(a), (c), and (e). However, the microstructure within dendrites cannot be distinguished among NOR, Oil-quenching, and De-MQ-Sct samples. Therefore, the microstructures were further characterized by SEM. Compared with Figures 4(b), (d), and (f), in addition to coarse eutectic carbides as a common feature, it can be clearly seen that the sizes of secondary carbide particles in the NOR and

Oil-quenching samples were close, and their average size is larger than that of De-MQ-Sct sample.

## B. Hardness and Toughness

The hardness distribution of the sample treated by the De-MQ-Sct process, Oil-quenching process, or NOR process was measured along a straight line through the center of sample. Figure 5 shows that the average hardness of the De-MQ-Sct sample reaches about 60 HRC, about 17 HRC higher than that of the NOR sample and about 4 HRC higher than that of Oil-quenching sample. Additionally, the hardness deviated from the average values are  $\pm 1$  HRC for De-MQ-Sct sample,  $\pm 2.6$  HRC for Oil-quenching sample, and  $\pm 3$  HRC for NOR sample, in which De-MQ-Sct sample exhibits the minimum deviated value of the hardness distribution. High hardness and/or small hardness deviation exhibit good wear resistance,<sup>[5]</sup> and thus the De-MQ-Sct samples imply better wear resistance than NOR and Oil-quenching samples. During De-MQ-Sct process, the high-chromium cast iron ball experienced multiple stages of air cooling after water quenching, which greatly reduces the temperature difference between surface and center. This effect can increase the homogeneity of microstructure and hardness, but cannot eliminate the difference of cooling rate between the surface and center of ball. The NOR sample exhibits the largest fluctuations of hardness, which is mainly attributed to the large hardness difference between carbides and pearlite.

Table II exhibits the impact toughness of samples treated, respectively, by De-MQ-Sct, Oil-quenching, and NOR processes. The average impact toughness value of three De-MQ-Sct samples is 12.6 J/cm<sup>2</sup>, being about four times as the NOR sample and twice as the Oil-quenching one. The above results indicate that high-chromium white cast iron treated by the De-MQ-Sct process can achieve the combination of the highest toughness and hardness.

The fracture morphologies of NOR, Oil-quenching, and De-MQ-Sct samples are shown in Figure 6. As seen from Figure 6(a), there are plenty of long and straight cleavage facets as main brittle feature. According to pearlite as majority of microstructure in the NOR sample, it reasonably believed that the long and straight cleavage facet probably forms at interface between cementite and ferrite in pearlite. In the Oil-quenching sample, there are considerable long and straight cleavage facets and dimples as main mixture feature of brittle and toughness. It should point out that the long and straight cleavage facet probably forms at interface between twin-type martensite plates based on the martensite as the majority of microstructure in

**Table I. The Volume Percents of Phases in the Samples Treated, Respectively, by Three Processes**

Process	Eutectic Carbide	Secondary Carbide	Pearlite	Retained Austenite	Martensite
De-MQ-Sct	16.1	13.0	13.8	12.2	44.9
Oil-quenching	17.4	9.2		8.5	65.1
NOR	19.7	7.3	73.0		

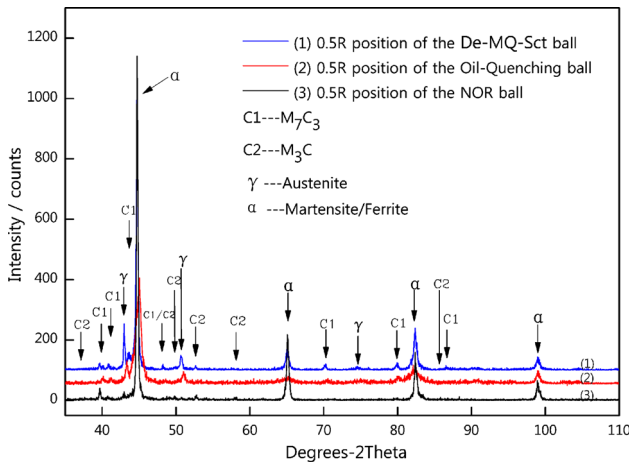


Fig. 3—XRD spectra of the De-MQ-Sct, Oil-quenching, and NOR samples at 0.5 R position.

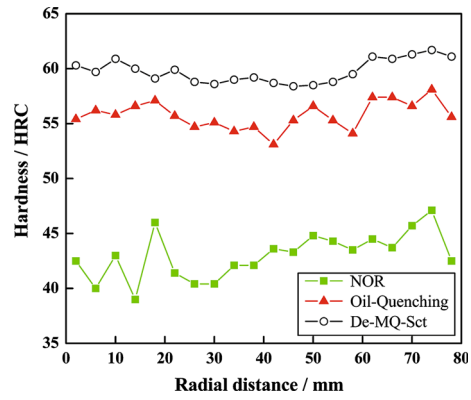


Fig. 5—The radial hardness of the balls treated, respectively, by three processes.

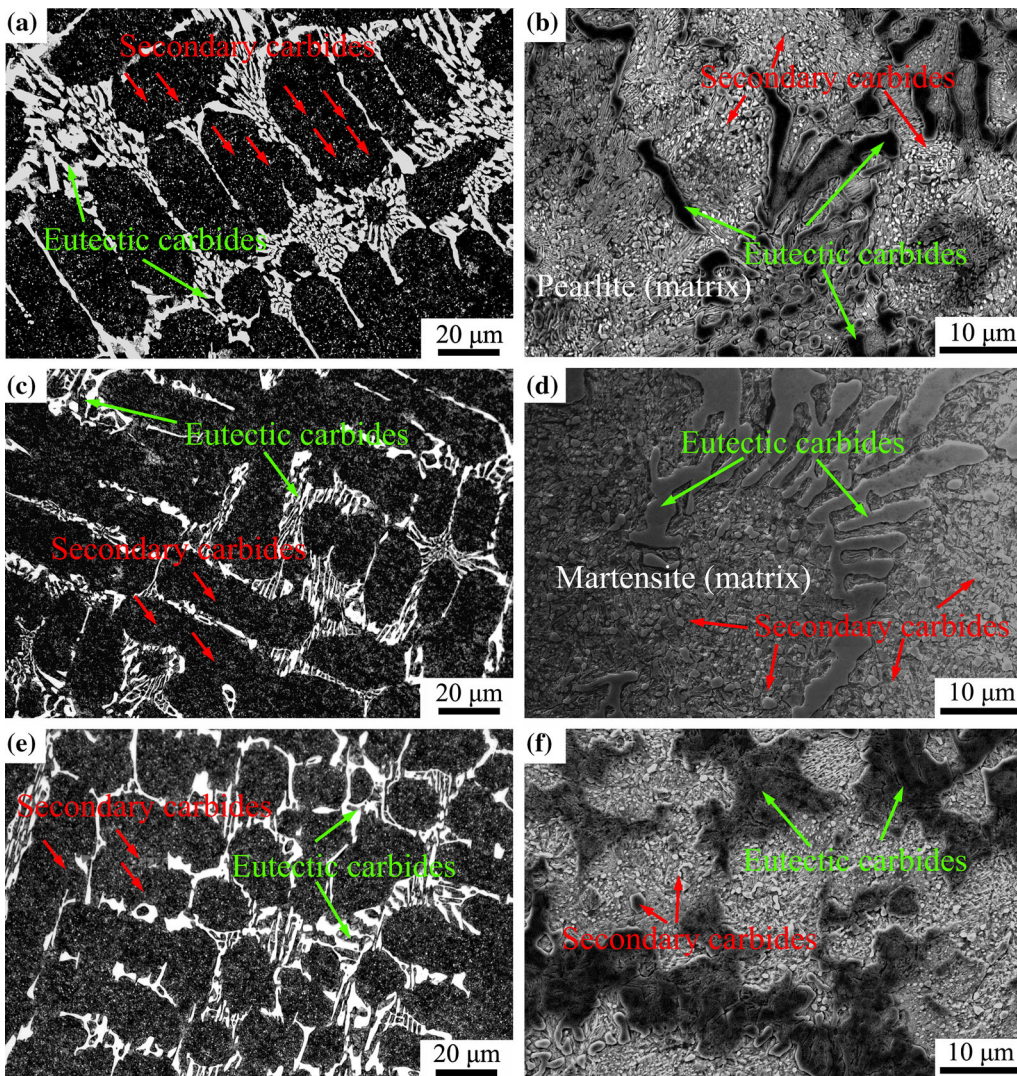


Fig. 4—Optical photographs (a, c, e) and SEM photographs (b, d, f) for NOR sample (a, b), Oil-quenching sample (c, d) and De-MQ-Sct sample (e, f).

Oil-quenching sample, rather than at interface between cementite and ferrite in pearlite since there is no pearlite in Oil-quenching sample. The fracture morphology of De-MQ-Sct sample demonstrates considerable deep dimples accompanying tearing ridges as main feature of toughness. Combined the analysis of microstructure, it is reasonably believed that tearing ridges are mainly attributed to the ductility phase-retained austenite and the dimples mainly result from large deformation of retained austenite or dislocation-type martensite around carbides in both Oil-quenching sample and De-MQ-Sct sample, and carbides in dimples are marked by arrows in Figures 6(b) and (c). In general, the fracture morphologies in three kinds of samples mentioned above are consistent with their impact toughness values.

### C. Wear Resistance

Figure 7 shows the results of wear tests at different positions of the balls for three kinds of samples, respectively. After the complete test sliding distance of 3670 m, the wear weight loss of NOR sample is about  $61 \times 10^{-4}$  g at the surface,  $66 \times 10^{-4}$  g at 0.5 R position and  $79 \times 10^{-4}$  g at the center of ball; the wear weight loss of Oil-quenching sample is about  $30 \times 10^{-4}$  g at the surface,  $40 \times 10^{-4}$  g at 0.5 R position, and  $54 \times 10^{-4}$  g at the center of ball; while the wear weight loss of De-MQ-Sct sample is about  $20 \times 10^{-4}$  g at the surface,  $22 \times 10^{-4}$  g at 0.5 R position and  $30 \times 10^{-4}$  g at the center of ball, being about one third for the NOR sample and one half for the Oil-quenching sample in three corresponding positions. It is clear that in three kinds of samples, De-MQ-Sct sample has the best wear resistance as a result of the highest hardness and toughness. Additionally, there is a trend for three kinds of samples that the weight loss of ball is the largest at the center, followed by the position of 0.5 R and finally the surface. The gradual increase of weight loss from the surface to center of ball is

attributed to the difference and inhomogeneity of microstructure produced by the different cooling rates between surface and center.

The widths of the worn surfaces of samples were also measured, as shown in Figure 8. For the samples treated by NOR, Oil-quenching and De-MQ-Sct processes, the worn surface widths were approximately 1350, 1150, and 850  $\mu\text{m}$ , respectively, and they are calculated, respectively, as 93.5, 67.0, and 36.4  $\mu\text{m}$  in depth based on the 5 mm diameter of grinding ball. These results indicate that the wear resistance of hypoeutectic high-chromium white iron is greatly improve by the novel De-MQ-Sct process compared with NOR and Oil-quenching processes.

The SEM images in Figure 9 show the details of worn surface after the wear tests of NOR, Oil-quenching, and De-MQ-Sct samples. It has been reported that the microgroove (microplowing) and microcutting chip are the two dominant mechanisms during the friction wear of white cast iron.<sup>[29]</sup> There are plenty of microgrooves at the worn surfaces in three kinds of samples, as shown

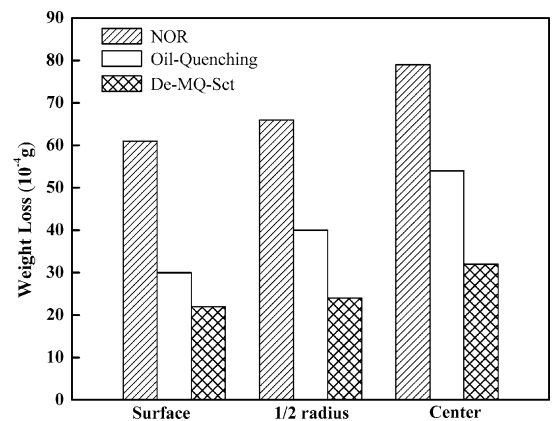


Fig. 7—Wear loss of three kinds of samples at different positions.

Table II. The Impact Toughness of the Samples Treated, Respectively, by Three Processes

Process	Sample 1 (J/cm <sup>2</sup> )	Sample 2 (J/cm <sup>2</sup> )	Sample 3 (J/cm <sup>2</sup> )	Average Value (J/cm <sup>2</sup> )
De-MQ-Sct	13.1	12.5	12.2	12.6
Oil-quenching	4.5	5.2	4.8	4.83
NOR	2.6	2.1	2.3	2.33

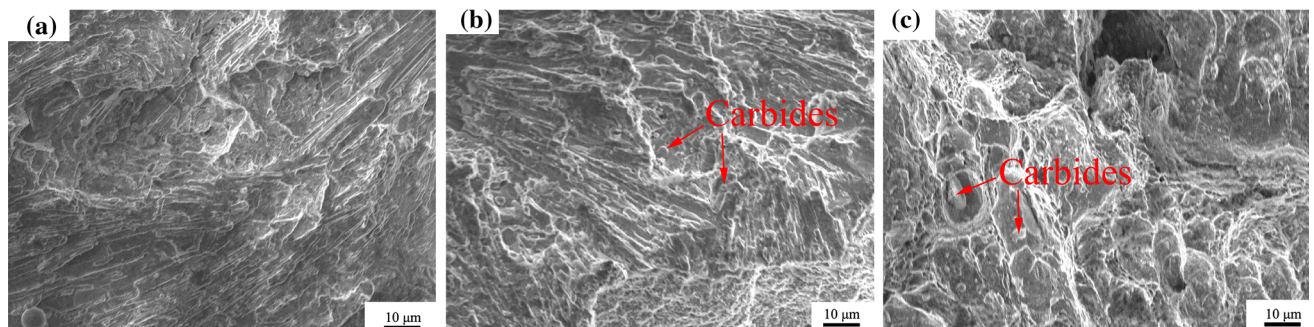


Fig. 6—Impact fracture morphologies of NOR sample (a), Oil-quenching sample (b), and De-MQ-Sct sample (c).

in Figures 9(a), (c), and (e). In microgrooves there are many microcutting chips, looks like fish-scale, as magnified images shown in Figures 9(b), (d), and (f). In magnified images of microgrooves, microcracks, and secondary carbides also can be clearly observed in

both NOR and Oil-quenching samples, as shown in Figures 9(b) and (d), but microcracks are hardly found in De-MQ-Sct sample, as shown in Figure 9(f). These features of microstructure also indicate the best wear resistance of De-MQ-Sct sample.

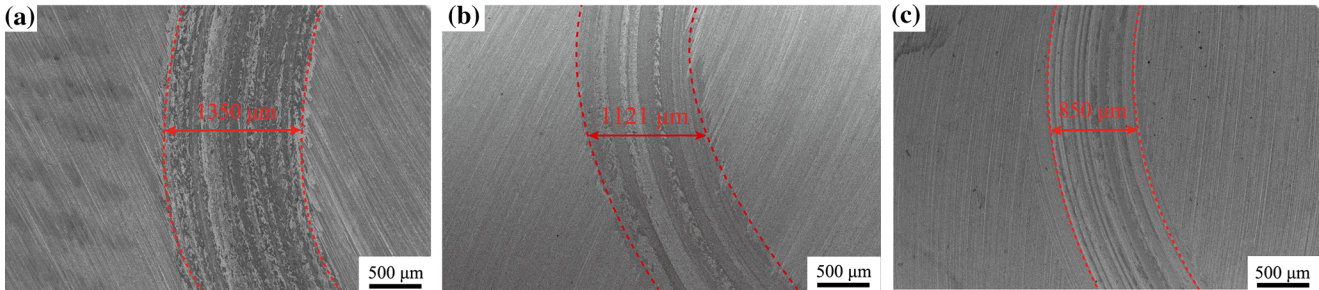


Fig. 8—The widths of the worn surfaces of samples treated, respectively, by different processes. (a) NOR, (b) Oil-quenching, and (c) De-MQ-Sct.

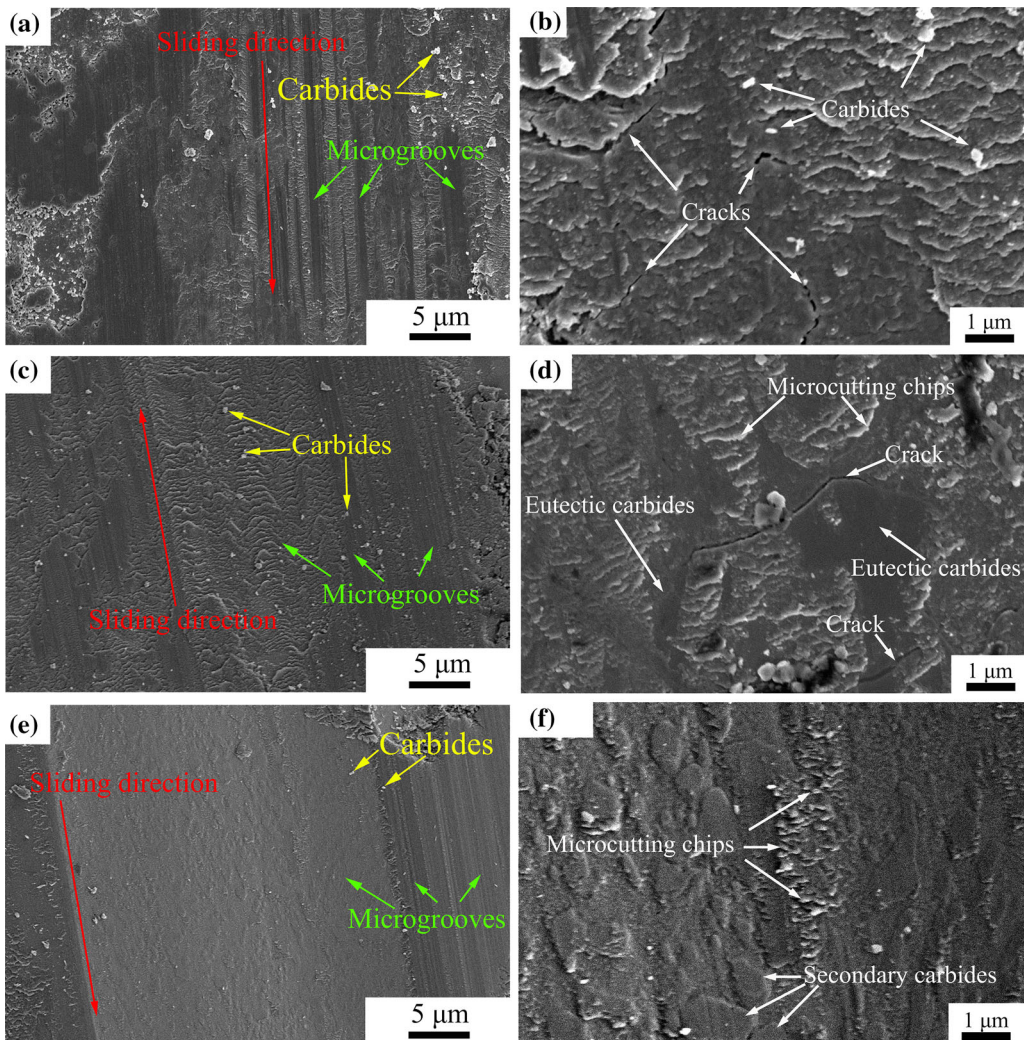


Fig. 9—The SEM images of the worn morphologies of samples treated by three processes. The microgrooves (a) and microcutting chips/microcracks (b) of NOR sample, the microgrooves (c) and microcutting chips/microcracks (d) of Oil-quenching sample, and the microgrooves (e) and microcutting chips (f) of De-MQ-Sct sample.

## IV. DISCUSSIONS

### A. Design Principle of Novel De-MQ-Sct Process

Novel De-MQ-Sct process is proposed in the basis of multicycle quenching-partitioning-tempering (MQ-P-T) process<sup>[26,28]</sup> after considering the disadvantages of destabilization treatment and sub-critical treatment applied in hypoeutectic white cast irons. In destabilization treatment a sample is heated to and held at 1223 K to 1373 K (950 °C to 1100 °C) to destabilize the austenite matrix by encouraging precipitation of secondary carbides, but secondary carbides easily grow at high temperature.<sup>[16]</sup> The precipitation reduces the carbon and chromium contents in the austenite and consequently raises the start temperature of martensitic transformation, and thus the martensitic transformation can occur at room temperatures<sup>[5]</sup> if cooling is fast enough to prevent pearlite formation. Obviously, rapid cooling is necessary for destabilization treatment. However, because white cast irons have casting defects and undesirable residual stress, at high quenching temperature rapid cooling is easily to cause the cracking. For the sake, white cast irons products are usually treated by air cooling (normalization) or oil cooling so as to avoid cracking, but air cooling usually cannot markedly improve the hardness and/or toughness of hypoeutectic cast irons in comparison with cast irons,<sup>[21]</sup> while oil cooling pollutes environment. Sub-critical heat treatment below austenitizing temperature [about between 873 K and 673 K (600 °C and 400 °C)] can overcome the disadvantage of cracking trend during rapid cooling in destabilization treatment. Compared with the destabilization heat treatment, adopting the sub-critical treatment can avoid distortion and fissuring of cast components and precipitate finer secondary carbides owing to its relative low treatment temperature.<sup>[19]</sup> However, sub-critical treatment needs long holding time to sufficiently precipitate secondary carbides so that maximum hardness can be obtained.<sup>[19,20]</sup> As a consequence, it is a challenge for white cast iron to avoid cracking and markedly improve mechanical properties by rapid cooling in shorter processing time. Novel De-MQ-Sct process can solve the issue. The core of novel De-MQ-Sct process is MQ-P-T process, which links the destabilizing treatment and sub-critical treatment. MQ-P-T process absorbs the idea of quenching and partitioning process (Q&P) process proposed by Speer *et al.* in 2003.<sup>[30]</sup> The Q&P process involves: a steel is quenched from austenitizing temperature to some temperature ( $T_q$ ) between martensite start ( $M_s$ ) and finish ( $M_f$ ) temperatures, and  $T_q$  is usually much higher than room temperature for low and medium carbon steels; and then is partitioned at or above  $T_q$  to accomplish the partitioning (diffusion) of carbon from supersaturated martensite into retained austenite so as to keep carbon-enriched retained austenite stable during subsequent cooling to room temperature. Obviously, Q&P process has two advantages<sup>[29,30]</sup>: (1) high  $T_q$  avoids the cracking trend during rapid cooling; (2) the partitioning of carbon from supersaturated martensite leads to more carbon-enriched retained austenite in

room temperature. Based on the Q&P process, we absorb the idea of Q&P process: the choice of quenching temperature ( $T_q$ ), and one after another developed quenching-partitioning-tempering (Q-P-T) process<sup>[31-34]</sup> and multicycle Q-P-T (MQ-P-T) process.<sup>[26]</sup> MQ-P-T process performed by alternate water quenching and air cooling has successfully been applied for the treatments of low/medium carbon forging or rolling products.<sup>[26]</sup> Obviously, MQ-P-T process can be developed to various processes for suitable for plenty of steels or irons when the austenitizing temperature and tempering temperature are set ones of a given steel or iron product. Meanwhile, MQ-P-T process can be suitable for various products with sizes range from several tens to hundreds millimeter by controlling the number of multicycle and time of both quenching in water and self-tempering in air, such as iron balls with diameter of 80 mm in this work and 42CrMo4 wind-electric spindle with spindle diameter of 540 mm, a length of 3600 mm and a weight of the about 15 t.<sup>[26]</sup> Of cause, for the latter as a large workpiece, the related quenching equipment and computer simulation combining measurement of cooling curves in various positions of workpiece are needed so that the optimized process can be obtained.<sup>[26]</sup> Therefore, such a flexibility of MQ-P-T process has wide applications.

In the De-MQ-Sct process, secondary carbide precipitation and martensitic transformation can continuously occur. During De-MQ-Sct process, the precipitation of secondary carbides in four stages lowers the content of carbon and chromium in austenite and raises  $M_s$ , which in succession promotes the martensitic transformation, meanwhile, martensitic transformation increases carbon content in austenite by the partition of carbon from supersaturated martensite into austenite, which in succession accelerates the precipitation of secondary carbides from supersaturated austenite. Such an interaction between carbide precipitation and martensitic transformation makes the secondary carbides and martensite matrix distribute in a whole sample, meanwhile, the martensite matrix in surface layer and sub-surface layer undergoes self-tempering, which leads to the relative uniform distribution of hardness in a whole sample. Besides, such an interaction is verified to markedly shorten process time by compared with sub-critical treatment.<sup>[21]</sup> It is worthy to point out that the interaction between carbide precipitation and martensitic transformation during De-MQ-Sct process cannot occur in the destabilizing heat treatment or sub-critical treatment because martensitic transformation only occurs during cooling after destabilizing treatment or sub-critical treatment, and thus the effect of martensitic transformation on the precipitation of secondary carbides does not occur. In short words, De-MQ-Sct process performed by alternate water quenching and air cooling has the following advantages:(1) multicycle quenching and self-tempering avoids the cracking trend; (2) multicycle partitioning of carbon results in the precipitation of more and finer secondary carbides; (3) multicycle partitioning of carbon results in the formation of more carbon-enriched retained austenite; and (4) the interaction between carbide precipitation and



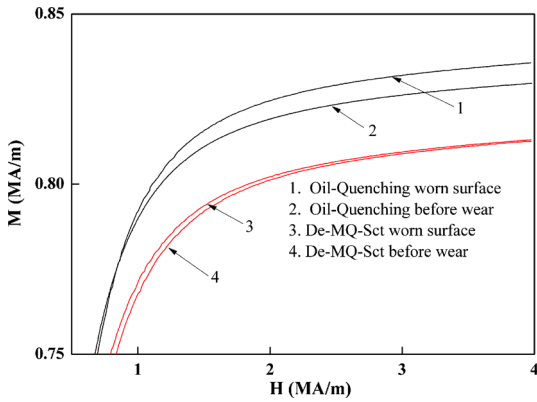


Fig. 10—The amount changes of martensite before and after wear test of De-MQ-Sct sample and Oil-quenching sample measured by PPMS.

martensitic transformation effectively shortens the time of heat treatment.

### B. Mechanism of High Wear Resistance

As mentioned above, the hardness and toughness of De-MQ-Sct samples are much higher than those of NOR and Oil-quenching samples, as shown in Figure 5 and Table II. The microstructural characterization indicates that the amount (16.1 pct) of eutectic carbides in De-MQ-Sct sample is close to that (19.7 pct) in NOR sample and that (17.4 pct) in Oil-quenching sample because their austenitizing temperature is same. Therefore, the high hardness of De-MQ-Sct sample is mainly attributed considerable martensite matrix and more and finer secondary carbides, while in NOR sample proeutectic austenite transforms to pearlite matrix, and in Oil-quenching sample although the amount of martensite is higher than that in De-MQ-Sct sample, the amount of secondary carbides is much less than that in De-MQ-Sct sample, moreover, their average size is much larger than that in De-MQ-Sct sample. The improvement of impact toughness of De-MQ-Sct samples, in addition to more and finer secondary carbides, is mainly attributed to considerable carbon-enriched retained austenite. TRIP effect can enhance ductility by martensitic transformation from retained austenite,<sup>[35,36]</sup> and whether TRIP effect can enhance the toughness of white cast iron is an issue we concern. The variations of martensite amount before and after wear tests of De-MQ-Sct sample and Oil-quenching sample were measured by magnetic method, rather than XRD which is not suitable for the measurement of the worn surface. Figure 10 shows the change of magnetization with magnetic field strength before and after wear test of De-MQ-Sct sample and Oil-quenching sample. It can be found that two curves of magnetization are almost overlapping before and after wear test of De-MQ-Sct samples when magnetization is close to saturation at 4 MA/m magnetic field strength. It means that the amount of martensite almost keeps unchanged after wear test, that is, martensitic transformation from retained austenite does not occur in wear loading. In

other words, the amount of retained austenite keeps unchanged after wear test. However, for Oil-quenching sample the saturation magnetization after wear test is higher than that before wear test. It means the increase of magnetic phase-martensite amount accompanying with the decrease of retained austenite in wear loading. The retained austenite in De-MQ-Sct sample is more stable than that in Oil-quenching sample, which results from higher carbon content in retained austenite by partitioning of carbon from martensite to retained austenite during De-MQ-Sct process. TEM observation confirms the above conclusion. Figure 11(a) is bright field (BF) image of the worn surface of De-MQ-Sct sample, and shows long and straight twin-type martensite plates and these plates are identified by selected area electron diffraction (SAED) pattern inserted in Figure 11(a). Figure 11(b) is BF image of hcp  $M_7C_3$  secondary carbides in the worn surface of De-MQ-Sct sample, and they are identified by SAED pattern inserted in Figure 11(b). These secondary carbides have relative large size with several tens micrometer, and thus they precipitate from austenite at high temperature. Dislocation-type martensite laths are demonstrated, respectively, by BF and DF image (Figures 11(c) and (d)). According to SEAD pattern in Figure 11(d), the orientation relationship (OR) between martensite and retained austenite is determined as N-W OR:  $(110)_\alpha // (\bar{1}\bar{1}1)_\gamma$ ,  $[00\bar{1}]_\alpha // [011]_\gamma$  and K-S OR:  $(110)_\alpha // (\bar{1}\bar{1}1)_\gamma$ ,  $[\bar{1}11]_\alpha // [011]_\gamma$ . Figures 11(e) and (f) are BF and DF images of retained austenite, respectively, in which retained austenite and nano-sized secondary carbides are at same time imaged by  $\bar{1}102_{M_7C_3}$  and  $\bar{1}\bar{1}1_\gamma$  in relative large objective aperture (see inserted SAED pattern in Figure 11(f)). It is worthy to point out that long and straight twin-type martensite plates is thermal-induced one forming during quenching because their lengths are over the size of retained austenite, and thus they are from the transformation of proeutectic austenite. Figure 12(a) is bright field (BF) image of the worn surface of Oil-quenching sample, and shows the twin-type martensite plates, retained austenite flakes. Twin-type martensite plates are further shown by DF image in Figure 12(b), and retained austenite in Figure 12(c), and their SAED pattern are shown in Figure 12(d). Comparing Figures 11(c) and 12(b), relative short twin-type martensite is strain-induced martensite by wear loading because they are limited in narrow retained austenite flakes. It can be found from a lot of TEM observation that the strain-induced twin-type martensite is not easy observed in the worn surface of De-MQ-Sct specimen, which is consistent with the results measured by magnetic method. Based on the above experimental results, two conclusions can be obtained: (1) strain-induced martensitic transformation in TRIP effect cannot enhance the toughness and wear resistance of white cast iron because twin-type martensite increases the source of crack initiation; (2) stable carbon-enriched retained austenite can markedly enhance the toughness and wear resistance of white cast iron because plastic retained austenite can decrease the cracks in the matrix by inactivating the crack tip and

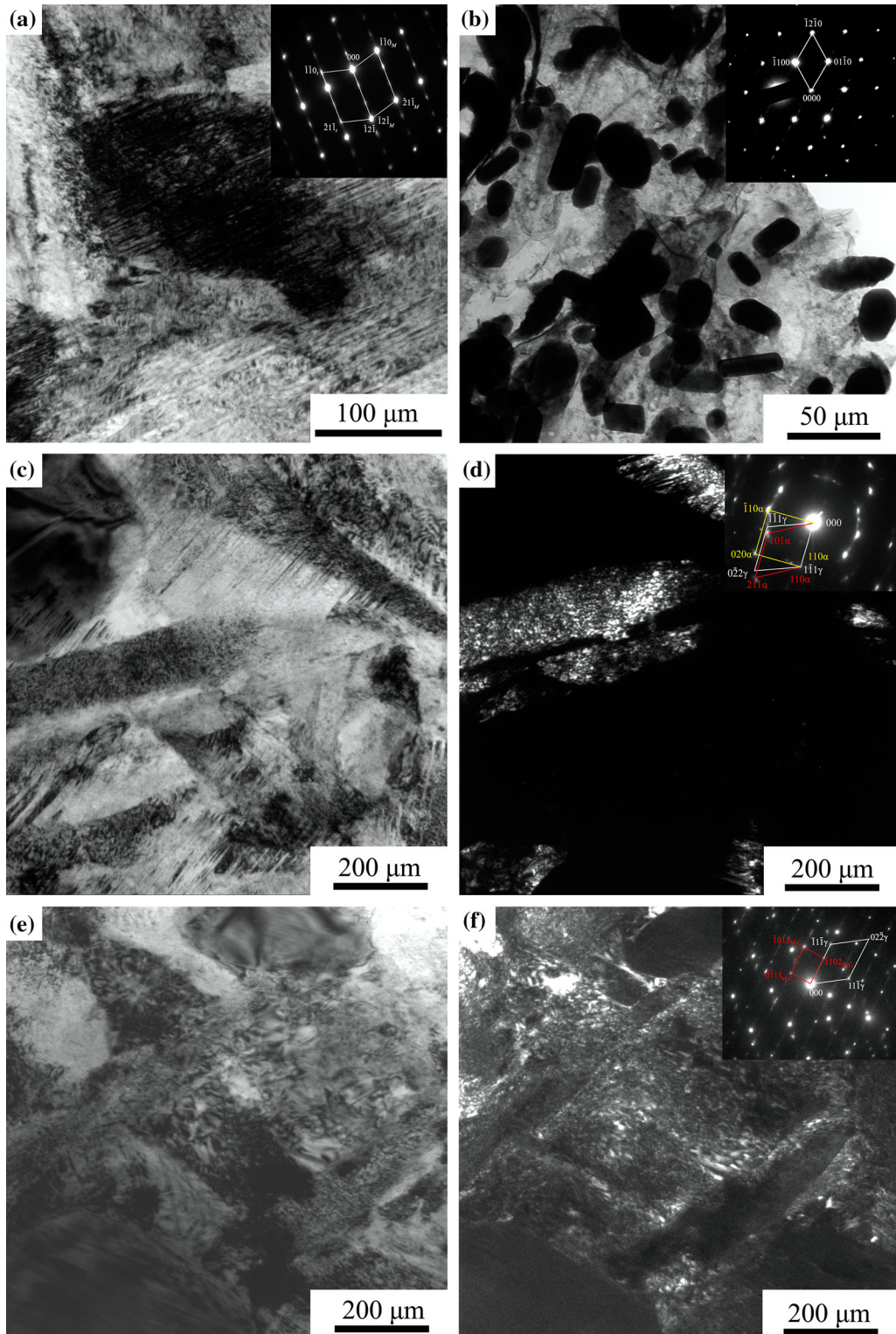


Fig. 11—The characterization microstructures in the worn surface of De-MQ-Sct sample. (a) Bright field (BF) image of twin-type martensite plates and SAED pattern inserted, (b) BF image of hcp  $M_7C_3$  secondary carbides and SAED pattern inserted, (c) BF image of dislocation-type martensite laths and twin-type martensite, (d) DF image of dislocation-type martensite, (e) BF image of retained austenite and secondary carbides, and (f) DF images of retained austenite and nano-sized secondary carbides and inserted SAED pattern.

inhibiting crack development,<sup>[4,15,23]</sup> moreover, the cracks grow either continuously in the austenite or trace a zig-zag path through interlocking martensite laths, which will require an increased energy for fracture.<sup>[30]</sup> So

far, the mechanism of high wear resistance for De-MQ-Sct white cast iron can be summarized as follows. The interaction between carbide precipitation and martensitic transformation during De-MQ-Sct

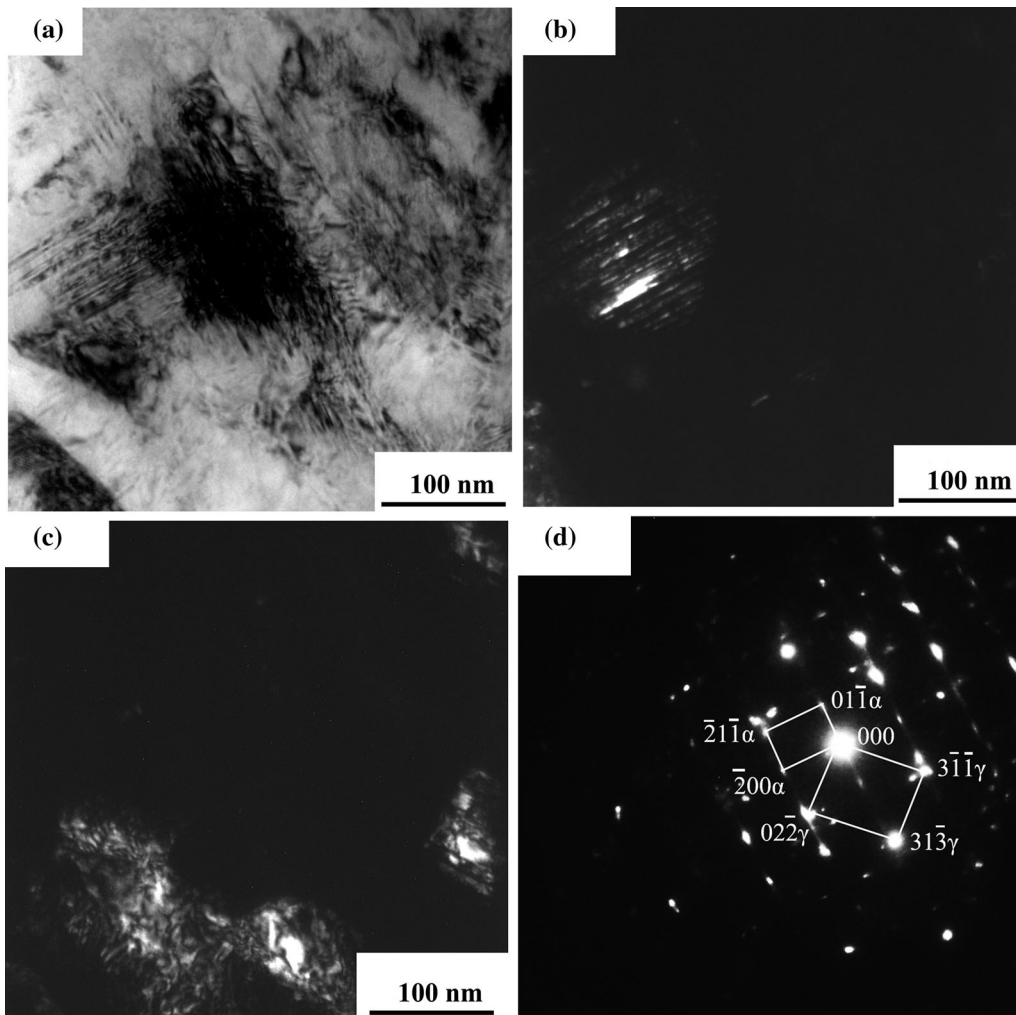


Fig. 12—The characterization microstructures in the worn surface of Oil-quenching sample. (a) BF image of twin-type martensite and retained austenite, (b) DF of twin-type martensite, (c) DF image of retained austenite, and (d) SAED pattern.

process leads to considerable fine secondary carbides and stable carbon-enriched retained austenite accompanying with high hardness and toughness. Therefore, considerable fine secondary carbides and stable carbon-enriched retained austenite play key roles in enhancing the wear resistance of De-MQ-Sct white cast iron.

## V. CONCLUSIONS

Fe-2.4C-12Cr cast balls with 80 mm diameter were treated by a novel De-MQ-Sct process and their mechanical properties and microstructures were characterized. Main conclusions are described as follows.

1. A novel De-MQ-Sct process was designed for Fe-2.4C-12Cr cast balls, both the HRC hardness and impact toughness of the De-MQ-Sct samples are markedly improved compared with those of the NOR sample and Oil-quenching ones, in which the average hardness increases by 17 HRC, and the average impact toughness increases by about four times comparing with NOR sample and by about 2 time comparing with Oil-quenching sample.
2. High hardness of De-MQ-Sct samples is mainly attributed to considerable fine  $M_7C_3$  secondary carbides. High impact toughness of De-MQ-Sct samples is mainly attributed to considerable stable carbon-enriched retained austenite and dislocation-type martensite matrix.
3. The weight loss of De-MQ-Sct sample is about one third of the NOR one and one half of the Oil-quenching one, and such a high wear resistance is mainly attributed to considerable fine secondary carbides and stable carbon-enriched retained austenite.
4. The strain-induced martensitic transformation in TRIP effect cannot enhance the toughness and wear resistance of white cast iron since twin-type martensite induced by strain is resource of crack initiation.
5. The De-MQ-Sct process performed by alternate water quenching and air cooling expands popular destabilizing treatment and sub-critical treatment, and the interaction between carbide precipitation and martensitic transformation during De-MQ-Sct process leads to considerable fine secondary carbides and stable carbon-enriched retained austenite.

## ACKNOWLEDGMENT

The work is financially supported by the National Natural Science Foundation of China (No. 51371117 and No. 51031001).

## REFERENCES

1. L.E. Svensson, H.K.D.H. Bhadeshia, B. Greftoft, and B. Ulander: *J. Mater. Sci.*, 1986, vol. 21, pp. 1015–19.
2. A. Neville, F. Reza, S. Chiovelli *et al.*: *Metall. Mater. Trans. A*, 2006, vol. 37A, pp. 2339–47.
3. J.T.H. Pearce and D.W.L. Elwell: *J Mater Sci Lett.*, 1986, vol. 5, pp. 1063–64.
4. A. Wiengmoon, T. Chairuangri, A. Brown, R. Brydson, D.V. Edmonds, and J.T.H. Pearce: *Acta Mater.*, 2005, vol. 53, pp. 4143–54.
5. M. Janssen, M.B. Van Leeuwen, M.F. Mendes de Leon: *Proceedings of the 14th European Conference on Fracture*, A. Neimitz *et al.*, eds., Emas Publications, London, 2002, pp. 617–25.
6. K.-H.Z. Gahr and D.V. Doane: *Metall. Trans. A*, 1980, vol. 11A, pp. 613–20.
7. C.K. Kim, S. Lee, and J.-Y. Jung: *Metall. Mater. Trans. A*, 2006, vol. 37A, pp. 633–43.
8. A. Bedolla-Jacuinde, M.W. Rainforth, and I. Mejia: *Metall. Mater. Trans. A*, 2013, vol. 44A, pp. 852–57.
9. X. Zhi, J. Xing, H. Fu, and Y. Gao: *Mater. Charact.*, 2008, vol. 59, pp. 1221–26.
10. X.H. Tang, R. Chung, C.J. Pang, D.Y. Li, B. Hinckley, and K. Dolman: *Wear*, 2011, vol. 271, pp. 1426–31.
11. Z. Liu, Y. Li, X. Chen, and K. Hu: *Mater. Sci. Eng. A*, 2008, vol. 486, pp. 112–16.
12. X. Chen and Y. Li: *Mater. Sci. Eng. A*, 2010, vol. 528, pp. 770–75.
13. C. Rodenburg and W.M. Rainforth: *Acta Mater.*, 2007, vol. 55 (7), pp. 2443–54.
14. A. Bedolla-jacuinde, S.L. Aguilar, and B. Hernandez: *J. Mater. Eng. Perform.*, 2005, vol. 14, pp. 149–57.
15. A. Wiengmoon, J.T.H. Pearce, and T. Chairuangri: *Mater. Chem. Phys.*, 2011, vol. 125, pp. 739–48.
16. H. Gasan and F. Erturk: *Metall. Mater. Trans. A*, 2013, vol. 44A, pp. 4493–5005.
17. C.P. Tabrett, I.R. Sare, and M.R. Ghomashchi: *Int Mater Rev.*, 1996, vol. 41, pp. 59–82.
18. J. Wang, C. Li, H. Liu *et al.*: *Mater. Charact.*, 2006, vol. 56 (1), pp. 73–78.
19. J. Wang, R.L. Zuo, Z.P. Sun, C. Li, H.H. Liu, H.S. Yang, B.L. Shen, and S.J. Huang: *Mater. Charact.*, 2005, vol. 55, pp. 234–40.
20. H.-H. Liu, J. Wang, B.-L. Shen, H.-S. Yang, S.-J. Gao, and S.-J. Huang: *Mater. Des.*, 2007, vol. 28, pp. 1059–64.
21. X. Jia, Q. Hao, X. Zuo *et al.*: *Mater. Sci. Eng. A*, 2014, vol. 618, pp. 96–103.
22. G. Laird, II and G.L.F. Powell: *Metall. Mater. Trans. A*, 1993, vol. 24A, pp. 981–88.
23. C.P. Tabrett and I.R. Sare: *Scr. Mater.*, 1998, vol. 12, pp. 1747–53.
24. I.R. Sare and B.K. Arnold: *Metall. Mater. Trans. A*, 1995, vol. 26A, pp. 1785–93.
25. A. Bedolla-Jacuinde, M.W. Rainforth, and I. Mejia: *Metall. Mater. Trans. A*, 2013, vol. 44A, pp. 856–72.
26. X.W. Zuo, N.L. Chen, F. Gao, and Y.H. Rong: *Int. Heat Treat. Surf. Eng.*, 2014, vol. 8, pp. 15–23.
27. X. Zhu, W. Li, H. Zhao *et al.*: *Int. J. Hydrog. Energy*, 2013, vol. 38 (25), pp. 10694–703.
28. S. Zhou, K. Zhang, N.L. Chen, J.F. Gu, and Y.H. Rong: *ISIJ Int.*, 2011, vol. 51, pp. 1688–95.
29. C.P. Tabrett and I.R. Sare: *Wear*, 1997, vol. 203, pp. 206–19.
30. J. Speer, D.K. Matlock, B.C. De Cooman, and J.G. Schroth: *Acta Mater.*, 2003, vol. 51, pp. 2611–22.
31. T.Y. Hsu: *Mater. Sci. Forum*, 2007, vol. 561, pp. 2283–86.
32. K. Zhang, W.Z. Xu, Z.H. Guo, Y.H. Rong, M.Q. Wang, and H. Dong: *Acta Metall. Sin.*, 2011, vol. 47, p. 489.
33. N. Zhong, X.D. Wang, L. Wang, and Y.H. Rong: *Mater. Sci. Eng.*, 2009, vol. A506, p. 111.
34. X.D. Wang, N. Zhong, Y.H. Rong, and Z.Y. Xu: *J Mater Res*, 2009, vol. 24, p. 261.
35. V.F. Zackay, E.R. Parker, D. Fahr, and R. Busch: *ASM Trans. Quart.*, 1967, vol. 60, p. 252.
36. D. Webster: *ASM Trans. Quart.*, 1968, vol. 61, p. 816.